Controlling Roof Beam Failures From High Horizontal Stresses in Underground Stone Mines

A. T. Iannacchione, Acting Deputy Laboratory Director
D. R. Dolinar, Mining Engineer
L. J. Prosser, Research Physical Scientist
T. E. Marshall, Engineering Technician
D. C. Oyler, Mechanical Engineer
C. S. Compton, Engineering Technician

National Institute for Occupational Safety and Health
Pittsburgh Research Laboratory
Pittsburgh, PA

ABSTRACT

The U.S., Australian, and United Kingdom coal and the Canadian hard rock mining industries have long recognized the significance of high horizontal stresses as a factor affecting the stability of roof and rib conditions in underground mines. Recently, a growing segment of the U.S. underground stone mining industry has also begun to recognize that horizontal stresses occur in some of its more than 90 mines. Considering the typically high strength and massive nature of limestone, this fact is a revelation in itself. High horizontal stresses produce extensive and sudden rock failures and, in some cases, resulted in injuries to mine workers. Through the years diverse control strategies have been proposed and experimented with. Reorientation of mine entries to reduce stress concentrations have proven successful and are widely accepted in practice. Other solutions, like rock reinforcement, are poorly understood and less accepted in practice. It is the purpose of this National Institute for Occupational Safety and Health (NIOSH) study to develop a better fundamental understanding of these ground control strategies under high horizontal stress conditions through a series of field and laboratory studies. To this end a design technique is presented which provides stone miners with a method for making stability assessments. The consequences of widening rooms, changing geology and horizontal stresses, and different rock bolts on roof beam failures are discussed.

INTRODUCTION

Excessive roof beam sag is considered the major cause of roof failure in U.S. underground stone mines. Roof beams can sag in response to gravity forces that pull subjacent beams away from overlying stable beams. Generally, these roof beams are formed in response to geologic characteristics, such as stratigraphic bedding, and are found in many stone mining provinces. Roof beams of varied thickness have been observed to span rooms ranging from 7 to 16 m (23 to 53 ft), some without any roof support. This can only occur if the beams are sufficiently strong/stiff, massive, and thick. Unfortunately, blasting fractures the immediate roof beam, adding to the frequency of roof failures.

The strength aspects of this failure criterion is generally easily met by most limestones. Typically, intact (solid) pieces of limestone are very strong, often having compressive strengths of 70 to 210 MPa (10.1 to 30.4 thousand psi or Ksi) and tensile strengths as high as 15 MPa (2.2 Ksi). Limestone has also been found to have a high stiffness, with elastic modulus (E) ranges from 13.8 to 41.4 GPa (2 to 6 million psi or Mpsi).

Not all limestone is massive; in fact, most limestone has horizontal layering that forms beams typically ranging from less than 0.15 to 0.6 m (0.5 to 2 ft) thick (Figure 1). Variations in roof beam thickness are caused by horizontal bedding planes of varying lengths and spacing. Some of these beams contain different numbers of vertical and subvertical discontinuities (vertical joints or fractures and subvertical crossbed planes). These fractures allow local sections of the immediate roof or rib to separate, forming prisms or wedges. These local wedge instabilities can suddenly fail without warning and are especially common in rib falls.

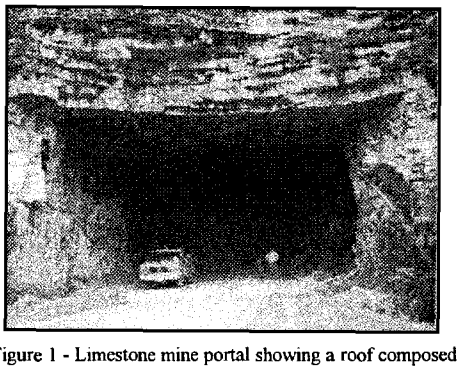

Figure 1 - Limestone mine portal showing a roof composed of numerous flat lying beams separated by bedding planes and ranging in thickness from 0.3 to 0.6 m (1 to 2 ft). It is estimated that greater than 95% of all underground stone mines have dips less than 10°.

When high horizontal stresses are applied to the ends of thin beams comprising the immediate roof, a buckling failure can occur. The approximate value of the critical load inducing the buckling failure can be determined by Euler's formula (Eq. 1):

$$P_{cr} = \frac{\pi^2 \cdot E \cdot I}{L^2} \qquad \text{(Eq. 1)}$$

where P_{cr} = Critical load
E = Elastic Modulus
I = Moment of Inertia
L = Length of beam

The value of the critical stress, σ_{cr}, corresponding to the critical load, P_{cr}, which induces buckling failure with respect to different end conditions is determined as follows:

$$\sigma_{cr} = \frac{\pi^2 \cdot E \cdot t^2}{12 \cdot L_e^2} \qquad \text{(Eq. 2)}$$

where σ_{cr} = Critical stress
t = Thickness of beam
L_e = Effective length of beam; for pinned end $L_e = 1*L$ and fixed end $L_e = 0.5*L$.

Using Euler's formula for both pin- and fixed-ended beams provides some general parameters related to stone roof beam stability. The strength of beams with different geometries and stiffnesses can be examined by plotting the critical stress at different beam slenderness ratios and elastic moduli. The critical stress for pinned and fixed-end beams is calculated by multiplying the beam length by 1 and 0.5, respectively. Figure 2 shows this relationship for three different elastic moduli: 13.8, 27.6, and 41.4 GPa (2, 4, and 6 Mpsi). The relative potential for buckling failure can be determined by evaluating the position of the calculated critical stress value. If the value plots below the strength/stiffness line, the beam has a low potential for buckling. Conversely, if the value plots above this line, the beam has a high potential for buckling.

As horizontal stresses are increased, roof beam deflection is induced. This deflection causes a maximum displacement in the center of a mined room and can be measured as roof beam sag. At the critical stress state, beam failure is thought to commence. The manner in which failure occurs has become a subject of much study. Roof beams can fail in shear as well as tensions. Multiple low angle shear failures have been recognized at several underground stone mines by the authors, as well as others (Emery, 1964; Parker, 1996; and Petersen, 1996). These failure surfaces are generally oriented perpendicular to the application of the load. Also, some roof beams have been observed to crack at their bottom center from the elevated tension levels in this portion of the deflecting beam.

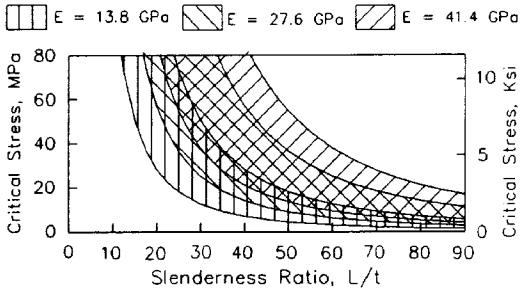

Figure 2 - Critical stress conditions for beams of various geometries and stiffnesses from Euler's formula.

These calculations clearly show that increasing the stiffness and/or the thickness of these beams is expected to dramatically increase their strength and hence the stability of the roof. Certain types of rock bolts can act to join thin layers, enhancing roof strength by increasing its flexural stiffness. Therefore, strategies to increase roof beam strength can minimize roof beam failures from moderate to high horizontal stresses and lessen the exposure of underground stone miners to hazardous conditions.

STRESS CONDITIONS IN U.S. UNDERGROUND STONE MINES

Because vertical stress is a function of the overburden, most underground stone mines are not deep enough to have high vertical stress problems. However, excessive levels of vertical stress are sometimes encountered in benching or multiple layer mining operations where pillar sizing and pillar positioning could produce local high stress concentrations. Unlike vertical stresses, horizontal stresses are directly related to overburden removal or tectonic forces especially in many near-surface conditions.

In the eastern U.S., it has been found that the magnitude of the horizontal stresses often exceeds the vertical stresses by a factor of at least two and can be much greater in shallow mines. Additionally, the ratio between the primary and secondary principal horizontal planes of stress ranges between 1.5 and 1.95 based on 26 measurements at 25 eastern U.S. coal mines (Mark and Mucho, 1994). These same measurements show that the orientation of the principal horizontal stress plane exhibits an ENE to E-W orientation in the northern Appalachian Basin. Because almost 20 underground stone mines operate within this same geologic province, it is expected that they will experience similar regional stress conditions. During 1995 and 1996, almost one-half of the underground stone mines in the U.S. were visited by the authors (Figure 3). High horizontal stress conditions were noted in western Pennsylvania, eastern Kentucky, West Virginia, and southwestern Virginia.

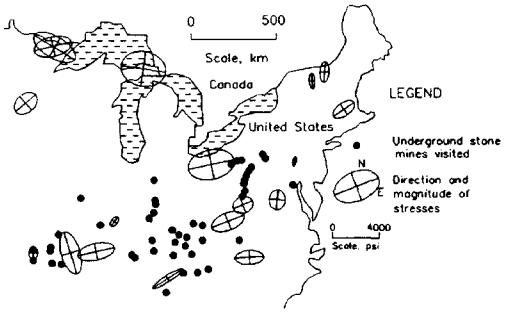

Figure 3 - Location of U.S. underground stone mines visited during this investigation and measurements of in situ stresses at nearby mines and quarries (Bickel, 1993).

Although these horizontal stress trends appear to be consistent over most of the eastern U.S., local variations can occur due to geologic structures (faults, igneous dikes, etc.), stratigraphic features (Parker, 1966), and topographic features (Molinda et. al, 1992). For example, Parker (1966) found that horizontal stress at the White Pine Copper Mine in the Upper Peninsula of Michigan varied from an apparent small degree of tension to 13.8 MPa (2,000 psi) of compression. Closer to a fault, stresses rose to 31 MPa (4.5 Ksi). In a deep limestone mine in Kentucky, Parker (1996) measured pressures in roof beams in excess of 96.6 MPa (14 Ksi). Therefore, local confirmation of stress field magnitude and orientation are necessary because stresses can change rapidly. This can be accomplished through measurement or by mapping the orientation of failure patterns developed in response to high horizontal stresses (stress mapping).

Stress mapping uses observational techniques to understand the local horizontal stress conditions. If high horizontal stress conditions exist, they will manifest themselves through several characteristic failure patterns. These patterns have been noticed and discussed by others (Parker, 1973; Gale 1986; and Mucho and Mark, 1994). Many of the same conditions noted by these researchers were observed by the authors at several underground stone mines. The following conditions were particularly noteworthy:

1. The strike of low-angle shear failure planes with associated rock powder oriented perpendicular to maximum horizontal stress direction.

2. Oval or elliptical roof failures oriented perpendicular to maximum horizontal stress direction (Figure 4).

3. Thin delaminated stone layers separated from the immediate roof and oriented perpendicular to maximum horizontal stress direction.

4. Joints and shear-type faults oriented parallel to maximum horizontal stress direction.

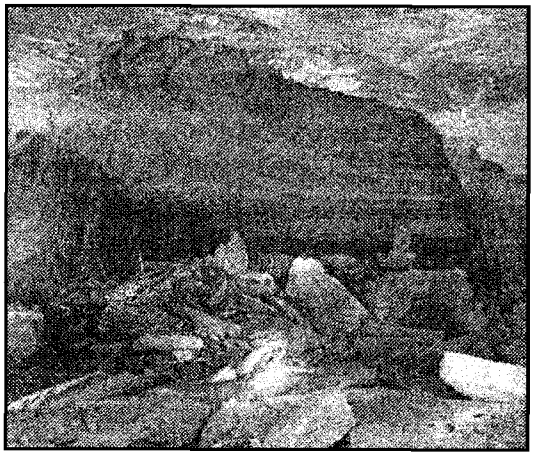

Figure 4. - If the roof is not reinforced properly with rock bolts, the beams can progressively fail higher into the roof until a stable roof beam is encountered. Here the roof fall has assumed an elliptical shape.

HIGH HORIZONTAL STRESSES AND ROOF BEAM BEHAVIOR

It has already been shown that the critical stress necessary to induce buckling failure within an Euler beam is dependent on the geometric characteristics and stiffness/strength of the beam. Unfortunately, the Euler beam is an oversimplification of the conditions found in most U.S. underground stone mines. For example, limestone roof beams are neither pinned nor fixed in the mechanical sense. More importantly, limestone roof strata typically contain multiple layers. The writers have found that many failures appear to originate in the lowest beams, or the beams closest to the mine opening (see case study discussed later in this report). This is probably due to the concentration of stresses in the lower beam and constraints to bending in the upper beams, and the fact that stress is highly concentrated in the lower beam at room corners.

Parametric Studies of Beam Thickness, Beam Strength, and Applied Horizontal Stress

Analyzing the complex interaction of multiple beams cannot be accomplished with analytical tools. Therefore, numerical models were employed to examine the interaction of far field applied stress conditions, local beam stiffness characteristics, and unique boundary properties. The finite difference code called FLAC was utilized because it contains realistic capabilities to model beam boundaries through the use of interfaces.

A grid 150 elements square was constructed that defined a bed of limestone 14 m (46 ft) in thickness and surrounded by weaker and thicker clay/shale member. The limestone has a stiffness of 27.6 GPa (4 Mpsi) surrounded with a clay/shale with a stiffness of 6.9 GPa (1 Mpsi). A room 13.7 m (45 ft) in width and 9.1 m

(30 ft) in height was excavated in the model to simulate a typical development entry used by many mines operating in the northern Appalachian Basin (Iannacchione, et al. 1995). The interface boundaries were placed at different locations above the mined rooms to simulate different roof beam thicknesses. A shear and normal stiffness of 10 GPa (1.45 Mpsi) and an angle of shearing resistance of 20° were assigned to each interface. Four different far-field horizontal stress fields were applied to the models, 3.45, 6,9, 13.8 and 27.6 MPa (0.5, 1, 2, and 4 Ksi), a range consistent with horizontal stress conditions found to exist in the northern Appalachian Basin.

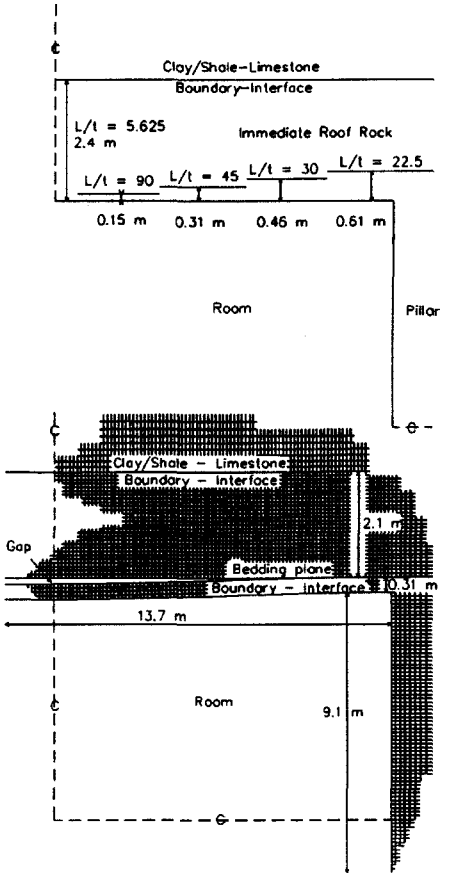

Figure 5 - Dimensions of five beams used in parametric investigations. At high horizontal stresses and slenderness ratios, the beams began to sag, creating a gap in the modeled roof.

The emphasis of these parametric investigations was to examine various shaped beams under varying regional horizontal stress conditions. In this study, five beam slenderness ratios were examined: 5.6, 22.5, 30, 45, and 90 (Figure 5). At high horizontal stress levels, the immediate roof beam began to sag, inducing gaps in the modeled roof. The location, areal extent, and thickness of these gaps are the most critical observational data available to identify potential roof instabilities.

All material models were elastic to conform with Euler's stress-based failure criteria and to simulate elastic-beam bending phenomena. Euler's stress-based failure criteria assumes that beam failure is initiated when critical stress initiates beam buckling. However, the elastic numerical model continues to bend the beam until the unbalanced forces dissipate through the finite difference grid through a process called relaxation. Failure conditions are considered to be stress-based, relying on the critical stress condition to define beam stability. Beam horizontal stress conditions were calculated as the average stress along a vertical plane cutting the center of the beam.

Plots of average maximum horizontal stress conditions for five different beam geometries and four applied horizontal stress conditions are shown in Figure 6. In this analysis, the critical stress is calculated for a material with a stiffness of 27.6 GPa (4 Mpsi) using a fixed-end condition. The fixed-end condition is thought to more closely represent the end conditions found in underground mines than the pinned-end condition.

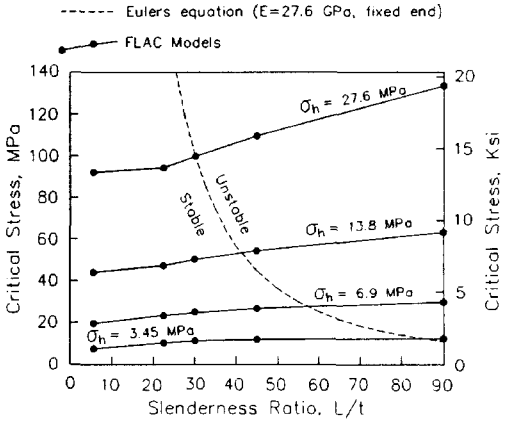

Figure 6 - Potential stability to buckling failure of differently shape roof beams with a varying horizontal stress field, ranging from 3.45 to 27.6 Mpa.

This new analysis supplies a very instructive view of the relationship between beam strength, beam geometry, and the regional horizontal stress field. If two of the conditions are held constant, the third can be altered to determine how it can potentially influence the onset of buckling failure. For example, if the mine is subjected to a 13.8 MPa (2 Ksi) horizontal stress field and the beam has a stiffness of 27.6 GPa (4 Mpsi), then a 0.3 m (1 ft) thick beam in a room 13.7 m (45 ft) wide (slenderness ratio=45) will plot in the unstable zone, indicating a high potential for buckling failure. Conversely, if the beam is 0.6 m (2 ft) thick, the intersection point of the 13.8 MPa and the 22.5 slenderness ratio conditions place this beam in the stable zone,

indicating a low potential for buckling failure. The following is a list of general trends identified from the parametric analysis:

1. At low regional horizontal stresses (< 3.45 MPa), beam buckling is highly unlikely in strong (high stiffness) rocks with slenderness ratios of less than 90. In this case, localized wedge failures due to gravity forces may be a much more significant factor.

2. At moderate regional horizontal stresses (6.9 to 13.8 MPa), beam buckling is likely to occur in most limestone rocks with intermediate stiffness characteristics and slenderness ratios of greater than 50.

3. At high regional horizontal stresses (> 27.6 MPa), beam buckling is likely to occur under almost any strength limestone rocks with slenderness ratios of greater than 30.

CONTROLLING HIGH HORIZONTAL STRESS THROUGH REINFORCEMENT: A CASE STUDY

Roof bolting has become an accepted means of maintaining roof stability in some stone mines with high horizontal stress conditions. In studying the role of reinforcement, the authors have recognized two basic approaches: 1) support the broken rock mass after the failed rock stabilizes, or 2) reinforce the roof beam to prevent buckling failure from occurring. Different roof support systems can be employed to achieve either of these objectives. The design guidelines presented here stress the second philosophy, i.e., prevention of roof beam buckling failure from occurring.

Available roof reinforcement systems consist of both active and passive types. An active system attempts to pulls the roof together by tensioning the bolt head. Conversely, a passive system relies on the sag of the roof beam to actively load the roof bolt. Two major considerations in deploying roof reinforcement are 1) suspension, pinning, or tying wedges or prisms of rock to a more competent member above or 2) reinforcing or beam building by joining individual thinner beams together to increase the effective beam thickness. In some cases where vertical jointing is common, blocks thickened by reinforcement can form the stable Voussoir Arch (Parker, 1996). Other important factors are bolt spacing, length, and capacity, all obviously tied to local stress, geologic, and mining considerations. The options available to achieve the above design issues are many. The types of products includes both mechanical and resin point anchor bolts, full-beam active and passive bolts (combinations of these two systems), and friction stabilizers, such as split-sets and swellex bolts, which rely on radial and frictional forces for anchorage. Because roof bolts in the underground stone industry are generally used on a spot basis, the selection process is complicated by the need to determine how, when, and where to use roof reinforcement. The following section will outline a case study where roof reinforcement was used to control high horizontal stresses.

Site Conditions

In-depth field studies were conducted at an underground operation in Pennsylvania mining the Loyalhanna Limestone. The limestone averages 21 m (70 ft) in thickness and is overlain by soft claystones and shales. Horizontal bedding planes are generally not laterally persistent in the Loyalhanna Limestone; therefore, it is sometimes necessary to create the roof line with blasting techniques. Immediate roof beam thicknesses were measured that ranged from 0.15 to 0.5 m (0.5 to 1.5 ft). Local practice is to leave approximately 2 m (6 ft) of limestone in the roof. This mine had experienced some problems with controlling a zone of failed roof that had a distinct directional trend to it. It had also periodically used roof support to control this ground with varying degrees of success. During this study, four types of support were used and their performance was evaluated: 1.59-cm (5/8-in) mechanical point anchor bolts, 2.22-cm (7/8-in) fully grouted resin bolts, 2.54-cm (1-in) torque-tensioned resin bolts, and 3.49-cm (1-3/8-in) friction stabilizer bolts (Figure 7). All bolts used in this study were 2.4 m (8 ft) in length.

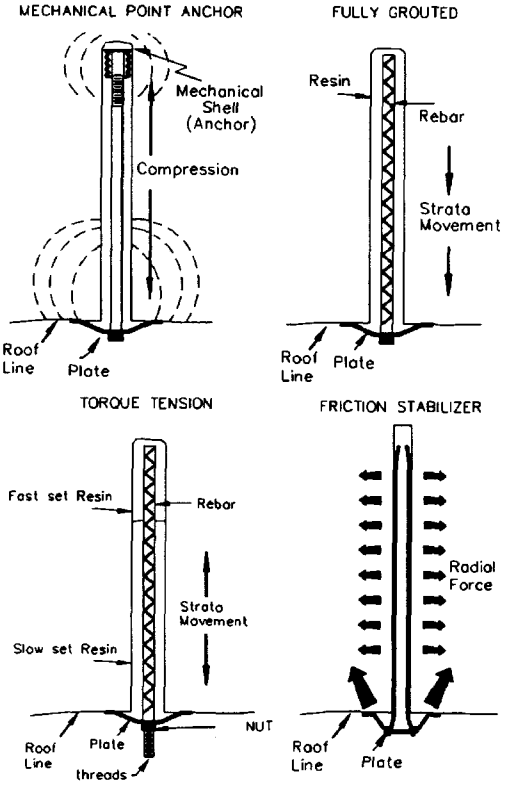

Figure 7. - Four common roof support systems: mechanical point-anchor, fully grouted resin, torque tension resin, and friction stabilizer bolts.

The characteristics of each of these supports are defined by their load-bearing capacity, stiffness, and postfailure characteristics. These characteristics were measured by conducting pullout tests (Figure 8) in the Greenbrier Limestone at NIOSH's Lake Lynn Underground Laboratory. The 1.59-cm (5/8-in) mechanical point anchor bolts displayed a low level of stiffness as the bolts elastically deformed approximately 0.5 cm (0.2 in), attaining a load of approximately 10 metric tons (11 tons). At this point, the bolts stretch and the anchors began to move or slip. These bolts displaced 14 cm (5.5 in) before failing. The 2.22-cm (7/8-in) fully grouted bolts are much stiffer, achieving approximately 22 metric tons (24 tons) of load at only 0.5 cm (0.15 in) of elastic deformation, primarily at the bolt head. One of the fully grouted bolts failed at this point; the other achieved over 4 cm (1.2 in) of plastic yield and gained an additional 10 metric tons (11 tons). The 2.54-cm (1-in) fully grouted torque-tension bolts were very stiff, achieving almost 35 metric tons (39 tons) of load at just over 0.5 cm (0.15 in) of elastic deformation. Both torque-tension bolts displayed very little plastic yield, displacing a total of only 1 cm (0.39 in) prior to failing between 36 to 37 metric tons (39 to 41 tons). The friction stabilizer bolts, i.e., split-sets and swellex bolts, rely on radial and frictional forces for anchorage. They are excellent at stabilizing wedges because of their ability to provide immediate resistance to deformation as a result of their high initial stiffness. This unique anchorage, however, does not provide very high load resistance, ranging between 4 and 12 metric tons (5 and 14 tons) (Scott, 1989; and Stillborg, 1992). These bolting systems can deform continuously for upwards of 5 cm (2 in) under constant load.

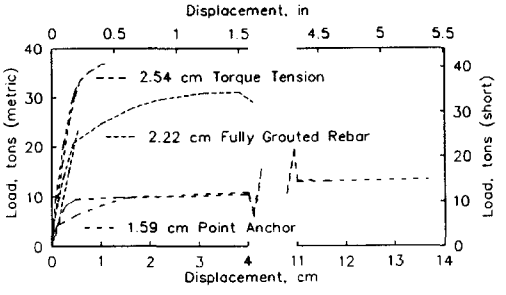

Figure 8. - Pull tests conducted on mechanical point anchor, fully grouted, and torque-tension bolting systems in limestone roof at the Lake Lynn Laboratory.

Measurements of Horizontal Stresses

Effective and efficient roof support systems require an understanding of how high horizontal stress conditions control the behavior of roof strata. An understanding of roof behavior can be accomplished by observational and measurement techniques used to analyze roof rock performance. In addition to stress mapping, 11 in situ stress measurements were conducted with the hydraulic fracturing method at the underground study site. The borehole where the tests occurred was examined with a fiber-optic probe (Figure 9). The roof in this area is composed of alternating sequences of limestone, claystone, and limey sandstones. The first 1.8 m (6 ft) contains a massive limestone with occasional bedding laminations. Between 1.8 and 2.7 m (6 and 9 ft) the first of numerous red claystone members occurs. Above these red bed members is another competent limestone unit. A relatively thick unit of red claystone is found between 4 and 5.2 m (13 and 17 ft). A massive calcareous sandstone unit is found high in the hole (5.2 to 5.9 m or 17 to 19.5 ft).

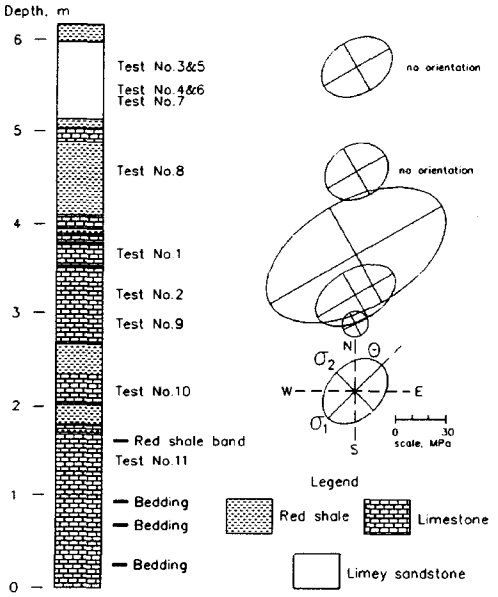

Figure 9. - Stress ellipses from six successful hydraulic fracturing tests within the roof of a Loyalhanna Limestone Mine.

Of the 11 tests, six produced enough data to estimate stress field orientations and magnitudes. Measurements of principal horizontal stress ranged from approximately 10 to 60 MPa (1.4 to 9 Ksi) with an average of approximately 25 MPa (3.6 Ksi). Of the five unsuccessful tests, three were due to our inability to propagate a fracture using pressures ot almost 69 MPa (10 Ksi). These are very high pressures and attest to the strong nature of the rock and the high in situ stress conditions. The other two unsuccessful tests were related to either problems with the fracture tool or hydraulic packers.

Of the six successful tests, stress field orientations could be determined from only four tests. Orientations were measured from the direction of vertical propagation produced during fracturing (Figure 9). All four vertical cracks propagated in the N45 to 65E direction. With the exception of test No. 9, all stress field values indicate that elevated horizontal stress conditions occur within this portion of the mine. In the case of test No. 1, the stress field was found to be extremely high. The reasons for this are still under investigation, but are undoubtedly related to the limestone beam-bending process, the location of the softened (fractured) zone within the immediate roof, the stress concentrations around the mine opening, and the variations in beam stiffness, i.e., stiffer layers store high levels of stress. The

orientations match reasonably well with the regional stress field found in other mines within this region (Figure 3).

Roof Failure Measurements

To understand better how these local horizontal stress conditions affect roof behavior, measurements of roof sag and the associated roof failure were made. The immediate roof began to fail in the middle of July approximately 90 m (300 ft) from the end of a previous directionally controlled roof fall. This original failure took on the appearance of a series of low-angled shear planes cutting or ripping the rock. The orientation of these planes was perpendicular to the orientation of the horizontal stress field as determined from previously discussed stress mapping and stress monitoring activities. Seven sag monitors were quickly placed along the projected failure trend. Two of seven monitors used the 20-point sonic probe; the other five were prototypes of a recently developed NIOSH monitor called the Remote Monitoring Safety System (RMSS) (Iannacchione et al., 1997).

Data collected from three of these monitors are shown in Figure 10. Monitor No. 7 collected sag measurements for almost 70 days prior to total roof collapse. During this time, the roof sagged in three distinct phases. The first phase was marked by a slow but steady sag in the lower roof beam. At approximately 40 days there was a sudden increase in the sag of the beam. The third phase indicated that the beam sag velocity lessened, but ended in total roof failure. A total of approximately 5 cm (2 in) of roof sag occurred prior to roof collapse. Data from monitor No. 3 showed a much different trend. Unlike monitor No. 7, this instrument was placed close to an existing failure; therefore, significant beam sag could have already occurred. The area began to "cut or rip" on July 26, rapidly extending the zone of failed roof. The roof associated with monitor No. 3 went from stable to unstable in a matter of 5 hours.

Monitor No. 4 was purposely placed slightly away from the main failure trend. The magnitude of sag measured from this instrument was 1/10 the magnitude of the instruments within the failure trend. However, these measurements did show that beam bending and associated shearing extended significant lateral distances on the order of 6 m (20 ft) from the fall's edge and 12 m (40 ft) from the center of the fall. This monitor also showed that while sag was initiated in the lowest beam, beam separations quickly moved much higher in the roof.

Rock Bolt Performance

Friction stabilizer bolts 2.4 m (8 ft) in length were installed in portions of the directional roof failure trend. Unfortunately, many of these bolts failed in the lower 1/3 of the bolt or at the location of the first major beam separation. Some of the bolts were stretched apart while others were sheared, indicating considerable shifting along the beam separations. In either case, these bolts were not of sufficient strength to resist the considerable beam sag.

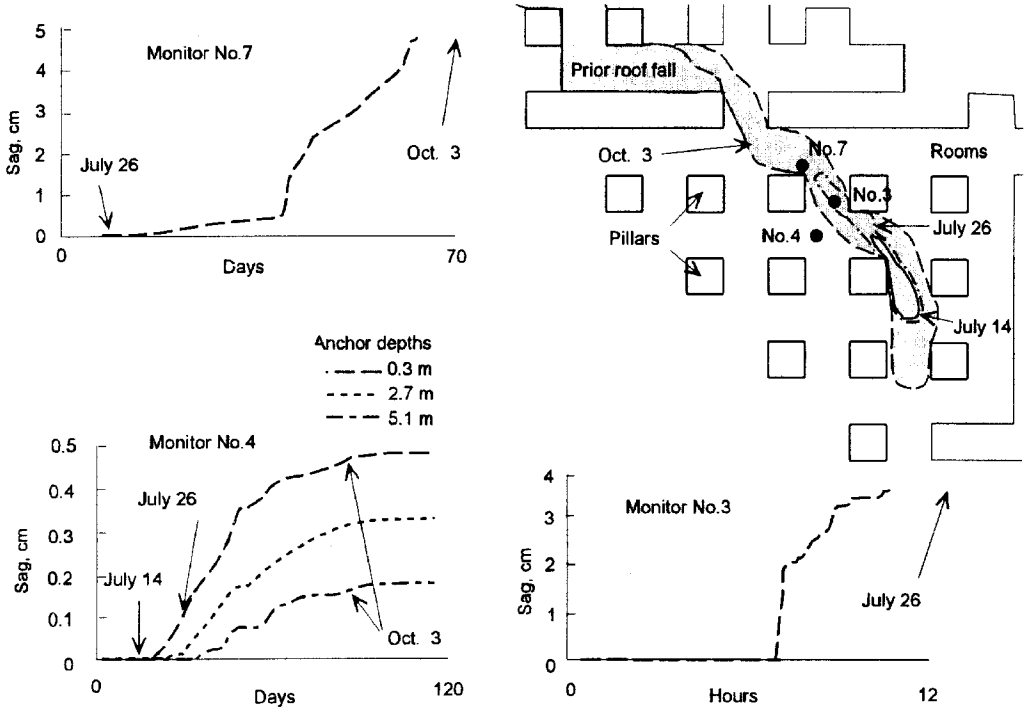

Figure 10. - Roof behavior associated with the large roof fall caused by high horizontal stresses.

The next bolt tried was a 1.59-cm (5/8-in) mechanical resin-assisted point anchor bolt 2.4 m (8 ft) in length. These bolts were similar in strength to the friction stabilizers, so they would have probably suffered from a similar fate. However, poor installation prevented this bolt from being placed in the high horizontal stress locations. The mechanical resin-assisted anchors were prone to spinners and could sometimes be pulled from their holes by mechanical scalers. It is thought that the limestone hole and the steel bar were both too smooth to allow the resin to bond well between the bolt and the rock, while the mechanical expansion shell seemed to have trouble anchoring into the limestone.

At this point, a new directionally controlled failure began to develop in another room. Mine management decided to try a much stiffer support, the 2.54-cm (1-in) torque-tension resin bolt. These bolts were quickly installed along the projected trend of the new directional failure zone. The fast-set resin along the upper bolt allowed the bolts to be tensioned to an estimated 5 metric tons (6 tons). This tensioning had the added benefit of pulling some of the loose lower beams together. Six RMSS's and three hollow inclusion cells were installed in this area to examine roof behavior. Additionally, a 10-m (30-ft) production bench was extracted to within 14 m (45 ft) of the bolted entry. Through the course of the 8-month monitoring period, stresses in the lower beams have changed as the roof was first loaded then unloaded as the bench extraction zone approached. Although the roof has shown some signs of localized cracking between the bolt heads, no beam collapses have occurred. Additionally, roof sag monitors have shown that very little sag has occurred in the bolted roof area. To this date, no torque tension resin bolts have failed.

Recently, the mine began using 2.22-cm (7/8-in) fully grouted resin bolts in new development areas. The reasons for this are twofold. First, the 2.54-cm (1-in) torque tension bolts must be manually inserted into the bolt holes. Because the bolts are very heavy, long-term usage could cause injury to the operator installing them. Second, because roof bolts are placed soon after mining, minimal separations exist in the roof. Hence, there is little need to tighten the beams together. To date, these bolts have performed without failure in areas where high horizontal stress conditions are thought to have existed.

ROCK REINFORCEMENT PERFORMANCE AND SELECTION

After reviewing the case study data, the question now is why some bolts performed better than others and what can we learn from this study to help in making the best selection in the future. In the case study, it seemed evident that stiffness and load capacity were the controlling factors in successful rock reinforcement performance. Clearly, rock reinforcement acted to strengthen the immediate roof by increasing the effective beam thickness. This enhanced reinforcement action was accomplished in our field test by higher capacity bolts, but it could have also been accomplished by closer bolt spacing. The critical point is that the thinner beams are tied together and act like thicker beams. Therefore, the critical stress needed to induce buckling is increased, decreasing the potential for buckling.

Although the concept of a stress-based failure criterion is straightforward, its application in controlling high horizontal stresses is not. After all, there is little evidence to suggest that rock reinforcement can significantly change the stress conditions within a roof beam. When rock reinforcement passes through adjacent layers, it does little to change the stresses that would have existed in the beam if the support were not there. This is true until failure or softening takes place. What the support does do is resist beam separation and reduce beam sag. Therefore, to analyze rock reinforcement performance it is necessary to utilize a deformation-based failure criterion.

Controlling Critical Roof Beam Sag Through Roof Reinforcement

To achieve a deformation based failure criterion, a critical sag magnitude needs to be established. It would be ideal to develop this critical sag magnitude based on many observations under a complete suite of geometric and strength characteristics. Unfortunately, there are limited experience and data in this area. Therefore, critical sag magnitudes need to be developed on a case-by-case basis. In this case study, 5 cm (2 in) of total sag preceded a major roof collapse. However, the lower beams began to fail prior to the main beam roof failure. It seems reasonable to assume that beam failure from buckling had begun in the lower beam at one-half of the total sag, or approximately 2.5 cm (1 in). Let's assume that this value is the critical sag magnitude and use it to assess the performance of unsupported and support roof beams.

In the parametric investigations discussed earlier, elastic beam sag occurred in beams with different slenderness ratios and under different horizontal stress conditions. The maximum vertical beam sag for each condition was calculated and displayed in Figure 11. If a match is made between conditions where a beam has a high potential for buckling, as defined by the critical stress failure criteria, and maximum vertical beam sag, then all conditions that produced more than 2.54 cm (1.0 in) of sag would represent a failure beam. This value correlates well with the sag magnitudes measured in the test site, validating the numerical model's performance.

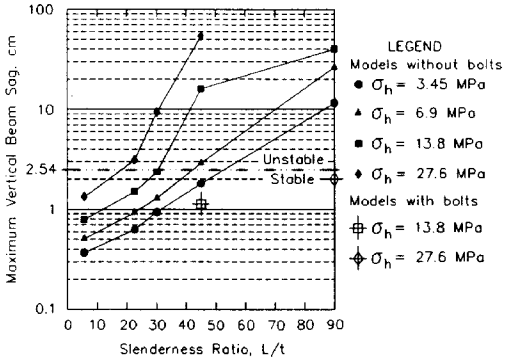

Figure 11. - Maximum vertical beam sag for several beam geometries and applied horizontal stress conditions with and without roof bolts.

To help examine the role played by rock reinforcement in controlling critical roof beam sag, numerical simulations were again used. This time, structural elements were placed in the model to simulate rock bolts. All four supports discussed earlier were evaluated. Material properties representative of these supports were chosen to simulate the material properties observed in the pull-out tests. Mechanical point anchor bolt performance was simulated by attaching the two end-points of the support elements to the finite difference grid. The two resin bolts were glued to their adjacent elements by placing a softer material with properties similar to resin grout between the modeled limestone and steel reinforcement. The friction stabilizer was modeled by removing the resin grout and allowing the steel to become attached directly to the modeled limestone.

These four rock reinforcement systems were run under two conditions presented previously where buckling failure was predicted by both the critical stress and critical displacement failure criteria. These two conditions represent a moderate failure potential, where horizontal stress was 13.8 MPa (2 Ksi) and the slenderness ratio was 45, and a very high failure potential, where the horizontal stress was 27.6 MPa (4 Ksi) and a slenderness ratio 90. All four bolts under both test conditions reduced maximum vertical beam sag to below the 2.5 cm (1 in) critical displacement failure criteria. That is approximately 1 cm (0.4 in) for the moderate failure potential conditions and 2.1 cm (0.8 in) for the very high potential failure conditions.

Selecting Effective Roof Reinforcement

Although the beams have been stabilized against buckling through rock reinforcement, some of the simulated bolts in the model were at or near their yield strength. Therefore it would be inappropriate to say that any kind of bolt could stabilize the beam under these conditions. In fact, our case study showed just the opposite. This is a direct result of the unique manner in which different bolts resist beam bending.

One way to evaluate the individual bolt performance is to examine their load distribution. For example, a mechanical point-anchor bolt compresses the beams between the anchor and the plate (Figure 7). Therefore, as the bolts resist sag the load is evenly distributed along the axis of the steel bar. The bar near the plate or in the threaded anchor section can stretch and fail when excessive loads are encountered. When this happens, the entire bolt loses all reinforcement value. The resin bolts distribute load in a very different fashion. Their resistance to sag is concentrated along that section of the bar where the beam separation is occurring. If the bar would happen to fail at this location, the rest of the intact bolt would still provide some resistance to separation at other locations in the bolted horizon. The friction stabilizers are unique in that they can gain pullout resistance in response to beam separation or lateral shifting. However, loss of contact with the host rock along the bolt axis can reduce its load-bearing capacity.

In addition to examining the influence of bolting on resisting beam sag, numerical simulations were used to evaluate the stability of the individual bolts. This was accomplished by determining the ratio of the axial load to the yield strength of each bolt at or near the beam's critical stress conditions (Figure 12). With a slenderness ratio of 45 and the horizontal stress field of 13.8 MPa (2 Ksi), the point anchor bolts were within 30% of achieving their maximum strength. Both fully grouted and torque tension resin bolts had more than 60% of their strength remaining, while one of the friction stabilizer bolts was at its yield strength. It is assumed that some bolts may fail when their yield strength is achieved and some additional yield takes place. In the case of the point anchor and friction stabilizer bolts, it may take additional sag to develop further plastic deformation before failure occurs. When the slenderness ratio was increased to 90 and the horizontal stress field was doubled to 27.6 MPa (4 Ksi), a different set of stability conditions was observed. The point anchor bolts were now at or close to yield. The resin bolts still had at least one-half of their strength remaining, while friction stabilizer bolts were in yield.

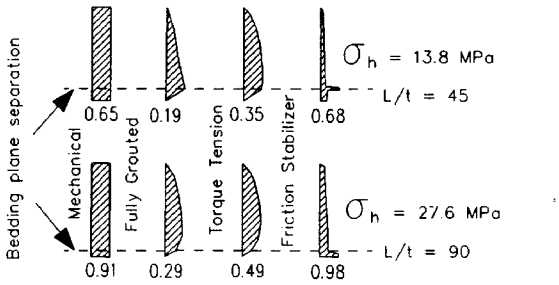

Figure 12. - Profiles of the average ratio of axial load to yield strength for four different bolt types placed under roof conditions that could potentially cause buckling failure of the lower roof beams.

The model results match well with field observations. These observations indicate that no resin bolts failed in the field test,

while considerable numbers of point anchor and friction stabilizer bolts failed. Bolt stability was directly related to load capacity. In some high horizontal stress conditions, the 6 to 12 metric tons (7 to 14 ton) of load capacity measured in the point anchor and friction stabilizer bolts was not enough to withstand loads generated by the deforming beams.

SUMMARY AND CONCLUSIONS

Roof beam behavior in underground stone mines with high horizontal stress conditions has been characterized using data gathered from the literature, mine visits, and field test sites. These roof beam behavior characteristics are:

1. Roof beams subjected to high horizontal stresses will deform or sag more than those only subjected to gravity loading.

2. Horizontal stresses are not dependent only on overburden. Shallow underground stone mines can have a wide range of horizontal stresses.

3. Horizontal stresses in western Pennsylvania, West Virginia, southwestern Virginia, and eastern Kentucky can be several times greater than the vertical stresses.

4. Observations of roof beam failures associated with high horizontal stresses have been recognized in several underground stone mines by the authors, as well as several other investigators.

5. Measurements of principal horizontal stress at one underground stone mine ranged from approximately 10 to 60 MPa (1.4 to 9 Ksi), with an average of approximately 25 MPa (3.6 Ksi) oriented in the ENE direction.

6. Buckling failure will occur once critical stress conditions exist within roof beams subjected to high horizontal stresses and may appear as tensile or shear failures

7. Critical stress conditions are influenced by beam stiffness/strength and geometry.

8. At one underground stone mine, approximately 5 cm (2 in) of total roof sag preceded a total roof collapse. It is assumed that roof layers began failing at approximately one-half of this total, or 2 to 3 cm (0.8 to 1.1 in).

9. Elastic numerical models agreed with field data when Euler's stress-based failure criterion was applied. These models were then used to examine the interaction of unique roof beam geometries with far field applied stress conditions.

10. Numerical models with roof bolts suggest that elastic beam sag could be reduced to 2 cm (0.8 in) or less at applied horizontal stress at or below 27.6 MPa (4 Ksi) and slenderness ratios of less than 90.

A design technique for layered limestone roof rock is presented based on the use of both stress- and deformation-based failure criteria. The stress-based failure criterion uses the Euler formula to evaluate the critical stress for buckling of beams of varying stiffness/strength and geometry subjected to different horizontal stresses. The stability of roof beams is also achieved using a deformation-based failure criterion calibrated with field data. The deformation-based failure criterion is used to evaluate the role of rock reinforcement in stabilizing roof beams. Roof bolt selection is based on bolt strength, length, and installation time. Conclusions drawn from this investigation are –

1. At low regional horizontal stresses (< 3.45 MPa), beam buckling is highly unlikely in strong (high stiffness) rocks with slenderness ratios of less than 90. In this case, localized wedge failures due to gravity forces may represent the more hazardous condition.

2. At moderate regional horizontal stresses (6.9 to 13.8 MPa), beam buckling or shearing is likely to occur in most limestone rocks with intermediate stiffness characteristics ands ratios of greater than 50.

3. At high regional horizontal stresses (>27.6 MPa), beam buckling is likely to occur under almost any strength limestone rocks with slenderness ratios of greater than 30.

4. Rock bolts act to reinforce the roof beams, increasing the effective thickness of the beams. These thicker layers produce roof beams that are more stable against buckling failure.

5. Two important rock bolt selection criteria under high horizontal stress conditions are bolt stiffness and load capacity.

The design technique presented provides stone miners a method for making stability assessments of roof beams in high horizontal stress conditions. The consequences of widening rooms, changing geology, and horizontal stresses can be examined. Also, provisions have been made for considering the role of rock reinforcement and selecting an appropriate roof bolt.

REFERENCES

Bickel, D.L., "Rock Stress Determinations From Overcoring - An Overview", U.S. Bureau of Mines Bulletin 694, 1993, pp. 58-62.

Gale, W. J., "The Application of Stress Measurements to the Optimization of Coal Mine Roadway Drivage in the Illawarra Coal Measures," Proceedings of the International Symposium on Rock Stress and Rock Stress Measurement, Stockholm, Sweden, September 1986, pp. 551-560.

Emery, C.L., "In Situ Measurements Applied to Mine Design", 6th Symposium on Rock Mechanics, Rolla, MO, 1964, pp. 218-230.

Iannacchione, A. T., T. P. Mucho, and L. J. Prosser, "Underground Limestone: An Overview of Ground Conditions," Proc. of the Environment, Safety, and Health Forum (National Stone Association), Nashville, Tennessee, Oct. 22-24, 1995, pp. 377-397.

Iannacchione, A. T. and L. J. Prosser, "Roof and Rib Hazard Assessment for Underground Stone Mines," SME Preprint 97-113, SME Annual Meeting, Denver, CO, Feb. 24-27, 1997, 5 pp.

Iannacchione, A. T., L. J. Prosser, D. C. Oyler, D. R. Dolinar, T. E. Marshall, and C. S. Compton, "Preventing Accidents Caused by Unrecognized Roof Beam Failures in Underground Stone Mines," National Occupational Injury Research Symposium, Morgantown, WV, Oct. 14-16, 1997, 10 pp.

Mark, C. and T. P. Mucho, "Longwall Mine Design for Control of Horizontal Stress," U.S. Bureau of Mines Special Publication 01-94, New Technology for Longwall Ground Control, 1994, pp. 53-76.

Molinda, G. M., K. A. Heasley, D. C. Oyler, and J. R. Jones, "Effects of Horizontal Stress Related to Stream Valleys on the Stability of Coal Mine Openings," U.S. Bureau of Mines RI 9413, 1992, 26 pp.

Mucho, T. P. and C. Mark, "Determining Horizontal Stress Direction Using the Stress Mapping Technique," 13th Conference on Ground Control in Mining, Morgantown, WV, 1994, pp. 277-289.

Parker, J., "Mining in a Lateral Stress Field at White Pine," Canadian Institute of Mining and Metallurgy Transactions, Vol. LXIX, 1966, pp. 375-383.

Parker, J., "How to Design Better Mine Openings: Practical Rock Mechanics for Miners," Engineering and Mining Journal, Part 5, December 1973, pp. 76-80.

Parker, J., "Everybody Goes Underground Eventually", Aggregate Manager, June 1996, pp. 30-35.

Petersen, G., Personal Communication, 1996.

Scott, J. J., "Roof Bolting - A Sophisticated Art," Coal, August 1989, pp. 59-69.

Stillborg, B., "Rock and Cable Bolt Tensile Loading Across a Joint," Swedish Rock Mechanics Symposium, Stockholm, Sweden, 1992.